15th Australasian Fluid Mechanics Conference
The University of Sydney, Sydney, Australia
13-17 December 2004

Flow visualisation of a pitching and heaving hydrofoil

Timothy C. W. Lau, Richard M. Kelso and Eyad R. Hassan

Department of Mechanical Engineering,
The University of Adelaide, North Terrace Campus, SA, 5005 Australia

Abstract

A fish-inspired heaving and pitching foil was investigated in a water tunnel using dye visualisation, at Reynolds numbers between 870 and 3480 (based on the chord length) and Strouhal numbers between 0.06 and 1.37. The variation of the wake pattern with respect to the Strouhal number was investigated. Three different wake regimes were observed - a drag wake, a transition wake and a thrust wake. The drag wake consisted of a combination of a regular Karman street and an array of 'primary' stop-start vortices, whereas the thrust wake consisted of a reverse Karman vortex street, commonly observed in swimming fish. The transition wake regime, which occurs at approximately $0.2 < St < 0.3$, is interpreted as a momentum balanced wake, where the thrust developed by the foil approximately balances its produced drag. This wake was observed to either consist of an in-line vortex street, or a paired vortex pattern.

Introduction

Interest in the swimming of aquatic animals took on a scientific edge with the publication of the now famous Gray's Paradox, which states that using standard steady-state fluid mechanics concepts, a swimming dolphin would have to produce more muscular power than was believed possible, or conversely, a swimming dolphin would have to be able to reduce its hydrodynamic drag. The latter possibility has large potential for application. Although the steady-state concepts used in Gray's Paradox have been shown to be inapplicable to swimming fish [7], the question remains whether swimming aquatic animals have capabilities of reducing drag (or of increasing efficiency) beyond what exists in man-made aquatic applications [2].

Although there are many forms of aquatic animals, here we concentrate on carangiform locomotion, or rather the interaction between the carangiform tails and the their wake, as the wake dynamics will provide clues as to how force production occurs during fish swimming. In many instances (such as [1]), carangiform tails (which generate the majority of the fish's total thrust) are modelled as heaving and pitching foils, and this is the concept adopted here.

Heaving and pitching foils have been demonstrated to produce thrust very efficiently (over 80% efficiency under certain conditions), and this occurs at a Strouhal number (St, see definition later) of approximately 0.25, where the wake is shown to be of a reverse von Karman vortex street form [1]. Interestingly, it appears that carangiform swimmers also swim at approximately the same St and produce the same wake form - the reverse Karman street [8, 10]. This would seem to suggest that fish "excite" the fluid-structure system at the system's "favoured" normalised frequency (i.e. St), analogous to a wave exciting a plate at its resonance frequency. At this juncture it also has to be noted that the commonly investigated flow past a stationary cylinder produces a "regular" von Karman vortex street wake, with a St of approximately 0.2 [6]. Taking into account the different parameter definitions, it is reasonable to wonder if the two St are linked.

The concept of a preferred operating condition is not limited to heaving and pitching foils - it also has been shown to some extent in the generation of vortex rings, whereby the vortex rings reach a maximum circulation at a non-dimensional 'formation time' of approximately 4, regardless of the geometry of their cylinder/piston setup [3]. As this formation time is loosely linked to St, it can be speculated that at $St \approx 0.25$, the circulation of the vortices developed by a foil may be maximised [9].

In other experiments, the effect of the body movements - as opposed to solely the tail movements considered thus far - is scrutinised. Lighthill [4] has shown mathematically that to produce thrust, the wavespeed of an undulating body (V) has to be slightly more than the speed of the free stream (U). The ratio of these two speeds ($\frac{V}{U}$) is of particular interest, as Triantafyllou *et al.* [9] quotes that $\frac{V}{U}$ values of approximate 1.2 - 1.5 give best results for reduction in turbulence intensity, and thus drag, for an undulating plate, and Muller *et al.* [5] show that the forward momentum of an undulating swimming fish is most considerable when $\frac{V}{U}$ is approximately 1.4. Furthermore, for the latter case, it can also be shown that at $\frac{V}{U} \approx 1.4$, the Strouhal number is approximately 0.25.

As can be seen, there are pockets of evidence which suggests that efficient force production develops when the system is excited at its preferred states. However, more evidence is needed before complete understanding is achieved. Therefore, the aim of this experiment is to investigate the effect of the Strouhal number on the wake dynamics of a heaving and pitching foil, to determine whether the foil could possibly produce efficient propulsion at $St \approx 0.25$, and why this St value is of significance. Particular attention will be given to the wake, as the experiments described above by Anderson *et al.* [1], and Muller *et al.* [5] show that the shift from the inefficient generation of forces to efficient generation of forces also corresponds to a shift in the wake form.

Experimental Setup

A NACA 0026 hydrofoil, with a chord length, c of 50mm and a span, l of 200mm (giving an aspect ratio of 4), is placed in a water tunnel with a working section of 1500mm x 500mm x 500mm. The foil is independently heaved and pitched harmonically, using a scotch yoke mechanism and a cam respectively, driven by two stepper motors (see figure 1). The heave amplitude, h_0 can be set to five discrete values, corresponding to $\frac{h_0}{c} = 0.0, 0.25, 0.5, 0.75, 1.0$. The amplitude of pitch angle θ_0, can be set to ten discrete settings by changing the offset of the cam, leading to pitch angle amplitudes from $\theta_0 = 0^0$ to $\theta_0 = 45^0$ in 5 degree intervals. The motion of the heave is sinusoidal, whereas the pitch motion is near-sinusoidal due to the effect of the shifting contact point on the cam-follower interface (maximum error $\approx 2\%$). The phase difference between the heave and pitch is defined as Ψ, and in these experiments is nominally set to 90^0.

The Strouhal number, based on the trailing edge excursion, is defined as $St = \frac{f \cdot A}{U}$, where f is the frequency (Hz), A is the peak to peak trailing edge excursion (consistent with [1]) and U is the free stream velocity. The frequency f of heaving and pitching can be directly controlled using a signal generator. The flow speed of the water tunnel can be set within a range of $U = 0 - 250$mm/s. Therefore, by setting all the above values beforehand, St can be determined prior to the experiments.

Dye is gravity-fed via a 1mm probe, which is fixed along the leading edge of the hydrofoil (see figure 1) at a depth corresponding to the mid-span of the foil. This allows the dye to be fed to both sides of the foil at the same time, and allows the dye probe to move with the foil when the foil is heaving. Food colouring diluted with the operating fluid from the water tunnel was used to visualise the flow, which in turn was recorded using a video camera (Sony DCR - TRV900E, 25 frames per second). The recordings are then digitally captured onto a computer for post processing.

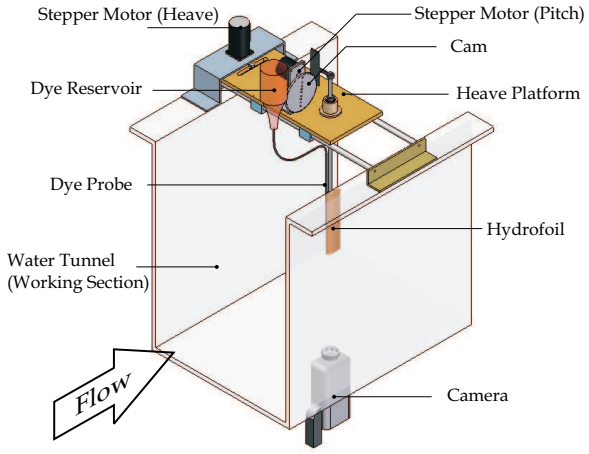

Figure 1: Experimental setup.

Results and Discussion

Altogether 113 different flow cases were investigated, captured in approximately 3 hours of digital video information (approximately 270000 frames). These flow cases consisted of combinations of different heave and pitch amplitudes, as well as different flapping frequencies and water tunnel flow velocities. The minimum and maximum *St* obtained were 0.06 and 1.37 respectively. The Reynolds number, *Re*, based on the foil chord ranged from 870 (for $U = 19.5$mm/s) to 3480 (for $U = 78$mm/s). All flow cases are cyclic, i.e., every cycle is identical to the previous cycle, however a few cases show asymmetry, whereby the upstroke and downstroke do not necessarily produce the same pattern of vortices (e.g. figure 4b). Nonetheless, the majority of the cases examined show symmetry, which would be expected since the motion of the foil is symmetrical as well.

A number of different wake patterns were observed. In particular we observe an in-line vortex wake pattern (figure 4c), a vortex pairing pattern (figure 4d) and a reverse Karman vortex street (figure 4e). The former two cases shed two vortices per cycle, whereas the latter case sheds four vortices per cycle. We also observe a "drag" wake pattern, whereby the wake pattern consists of a regular Karman vortex street which is slightly rotated from the streamwise axis (figure 4a). Many cases examined also show signs of additional vortices, which we denote "tertiary vortices". Figure 2 shows a reverse Karman wake with the clear existence of tertiary vortices. These vortices, which are usually shed between the half cycles, are differentiated from the vortices shed at the ends of the half cycles, which we call the "primary" vortices. The primary vortices are almost always noticeably stronger than the tertiary vortices.

The existence of the primary vortices can be explained using classical wing theory. The primary vortices are simply a combination of the stopping vortex of the previous half cycle, and the starting vortex of the subsequent half cycle, and hence they

Figure 2: Tertiary vorticity ($St = 0.51$).

are sometimes called start-stop (or stop-start) vortices. On the other hand, tertiary vortices are generated due to the instability of the shear layer near at the trailing edge of the wing - an area where the velocity gradients are high. Intuitively, the experiments also show that more tertiary vortices are produced at higher flapping speeds ($= f \cdot A$). We also define the secondary vortices, which are the vortices that are shed in the wake of an unforced or mildly forced drag producing body (see figure 3).

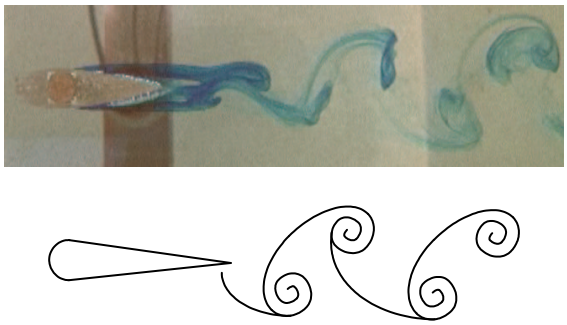

Figure 3: Secondary vorticity ($St = 0$).

In general, the differing wake patterns presented in figure 4 can be arranged into three different wake regimes - a drag wake, a transition or balanced wake and a thrust wake (see figure 5). The transition from a drag wake to a thrust wake occurs via the transition or balanced wake, and is strongly dependent on *St*. At low *St* (<0.2), the foil produces a wake indicative of drag - generally producing a pattern of the regular Karman street form. At very low *St* (<0.1), and at low to moderate heave amplitudes, the wake consists of a phase-rotated regular Karman street wake, whereby the vorticity is generated at the leading edge of the wing (figure 4c). At large heave amplitudes ($\frac{h_0}{c} = 1.0$), the pattern becomes complex and will be discussed in later publications.

Within this drag regime exists a wake pattern that is unexpected - an asymmetrical wake pattern (see figure 4b), which occurs at approximately $0.1<St<0.2$. This wake pattern consists of a pair of counter rotating vortices, plus an additional vortex per cycle. This asymmetry is cyclic, but the initial onset of the asymmetry is random. This asymmetrical wake pattern is also seen in experiments with oscillating cylinders [11], which the authors call the "P+S" (Pair + Single) vortex mode. This asymmetry is attributed to the generation of secondary vortices, which combine with the primary stop-start vorticity shed at the trailing edge of the wing. The vortex shedding frequency is synchronised with the flapping frequency of the wing, however there is a phase difference between the generation of these vortices, such that one drag vortex is shed freely into the wake while the other combines with the start-stop vortex, generating the pattern shown in

figure 4b. At slightly higher St, the competition between the two modes of vortex generation is balanced, either producing an in-line wake pattern or a vortex pairing pattern; this wake regime is called the balanced or transition wake regime (discussed below).

The balanced or transition wake regime occurs in the range $0.2 < St < 0.3$, where the wake shows evidence of an approximate momentum balance. This occurs when the drag forces on the wing balances the thrust produced by the wing. For this case, neither a momentum deficit nor a momentum surplus should be observed in the wake, and the wake patterns reflect this. Two wake patterns are observed in this St band; the first is the in-line wake pattern (see figure 4a), whereby two counter rotating vortices are shed along the centreline per cycle. The second wake pattern is the vortex pair pattern, whereby two pairs of counter rotating vortices are shed per cycle (figure 4d). Both wake patterns appear to be combinations of regular vortex shedding due to drag and the start-stop vortices shed at the trailing edge, following the asymmetrical case discussed above. The in-line wake pattern occurs when the start-stop vortices combine with the drag vortices of the same sign - therefore only generating two vortices per cycle. On the other hand, the vortex pair pattern occurs when the start-stop vortices and the drag vortices do not combine immediately - they are formed and shed separately. The arrangement and axial alignment of these shed vortices in both cases suggest that there is little momentum excess or deficit in the wake. Hence, it is likely that the wing is generating large side forces, but little thrust or drag. The strength of these vortices should be proportional to the magnitude of the side forces, which do not contribute to useful work.

At $St > 0.3$, the wake pattern consists of a reverse Karman street, indicating that the foil is generating forward thrust. Evidence of the development of thrust is also provided by the shed tertiary vortices, which are accelerated away from the foil when they enter the jet region of the foil - a phenomenon not observed in the other two wake regimes. As St increases, so does the apparent strength of the primary vorticity and, we expect, the magnitude of thrust. This flow regime also shows the greatest tendency to produce tertiary vortices.

The variation of the wake patterns with respect to St is summarised in figure 5, which is plotted against the maximum angle of attack of the wing. This angle is calculated from both heave and pitch angle amplitudes. The plot allows the direct comparison to the wake map produced by Anderson *et al.* [1], at $Re = 1100$. There are some major differences between the two plots. Firstly, Anderson *et al.* do not observe a transition regime at $0.2 < St < 0.3$. At this St range they observe a reverse Karman street. Secondly, they do not observe an in-line wake pattern, and the vortex pairing pattern they observe occurs either at high angles of attack ($> 50^0$) at all St, or at $St > 0.5$ at all angles of attack above 10^0. The first difference can be accounted for by the fact that the wake map produced by Anderson *et al.* is only for high heave values ($\frac{h_0}{c} = 1.0$), whereas the wake map produced here is for all heave values. In our study, high heave values account for five out of the six cases where a reverse Karman street is observed within the transition regime. The second major difference is, so far, inexplicable. Nevertheless, the results of Anderson *et al.* do indicate that at $St < 0.2$, low or negative thrust (drag) develops on the foil, with good agreement with the results presented here.

In general, our results indicate that, at $St < 0.2$, the secondary, or vortex shedding mode dominates the flow, and the foil generates drag. As St increases, the influence of the flapping increases, and at a certain point the relative influence of both the flapping and the vortex shedding is balanced, and both vortex generating modes are phase-locked. This occurs approximately at $0.2 < St < 0.3$, and it appears that little or no nett thrust or drag is developed. At $St > 0.3$, the flapping dominates the flow and the foil develops nett thrust. Therefore, to maintain steady propulsion, the parameters of the flapping foil have to be chosen such that $St \approx 0.25$, where the thrust and drag developed by the foil is balanced. This concurs with the observation that steadily swimming fish swim approximately at $St = 0.25$ [8]. However, there is no proof, as yet, that efficient propulsion can be developed at this St. The next part of our study, which will include laser imaging, will eventually allow the measurement of the wake parameters (most notably the strength of the primary vortices, and the geometry of the wake patterns), which would potentially provide important information regarding the generation of the wake vortices and also provide clues whether fish do in fact, swim with exceptional efficiency.

Conclusion

Flow visualisation of a heaving and pitching hydrofoil has revealed different wake patterns at various Strouhal numbers. These wake patterns can be classified into three regimes - a drag regime, a transition or balanced regime and a thrust regime. The transition regime occurs approximately at $0.2 < St < 0.3$, the St band at which fish have been observed to swim steadily.

References

[1] Anderson, J. M., Streitlien, K., Barrett, D. S. and Triantafyllou, M. S., Oscillating foils of high propulsive efficiency, *Journal of Fluid Mechanics*, **360**, 1998, 41–72.

[2] Barrett, D. S., Triantafyllou, M. S., Yue, D. K. P., Grosenbaugh, M. A. and Wolfgang, M. J., Drag reduction in fish-like locomotion, *Journal of Fluid Mechanics*, **392**, 1999, 183 – 212.

[3] Gharib, M., Rambod, E. and Shariff, K., A universal time scale for vortex ring formation, *Journal of Fluid Mechanics*, **360**, 1998, 121–140.

[4] Lighthill, J., *Mathematical Biofluiddynamics*, Society for Industrial and Applied Mahematics, Pennsylvania, 1975.

[5] Muller, U. K., Stamhuis, E. J. and Videler, J. J., Riding the waves: the role of the body wave in undulatory fish swimming, *Integrative and Comparative Biology*, **42**, 2002, 981 – 987.

[6] Nakamura, Y., Vortex shedding from bluff bodies and a universal strouhal number, *Journal of Fluids and Structures*, **10**, 1996, 159–171.

[7] Schultz, W. W. and Webb, P. W., Power requirements of swimming: Do new methods resolve old questions?, *Integrative and Comparative Biology*, **42**, 2002, 1018 – 1025.

[8] Triantafyllou, G. S., Triantafyllou, M. S. and Grosenbaugh, M. A., Optimal thrust development in oscillating foils with application to fish propulsion, *Journal of Fluids and Structures*, **7**, 1993, 205–224.

[9] Triantafyllou, M. S., Techet, A. H., Zhu, Q., Beal, D. N., Hover, F. S. and Yue, D. K. P., Vorticity control in fish-like propulsion and maneuvering, *Integrative and Comparative Biology*, **42**, 2002, 1026 – 1031.

[10] Triantafyllou, M. S., Triantafyllou, G. S. and Yue, D. K. P., Hydrodynamics of fishlike swimming, *Annual Review of Fluid Mechanics*, **32**, 2000, 33 – 53.

[11] Williamson, C. H. K. and Roshko, A., Vortex formation in the wake of an oscillating cylinder, *Journal of Fluids and Structures*, **2**, 1988, 355 – 381.

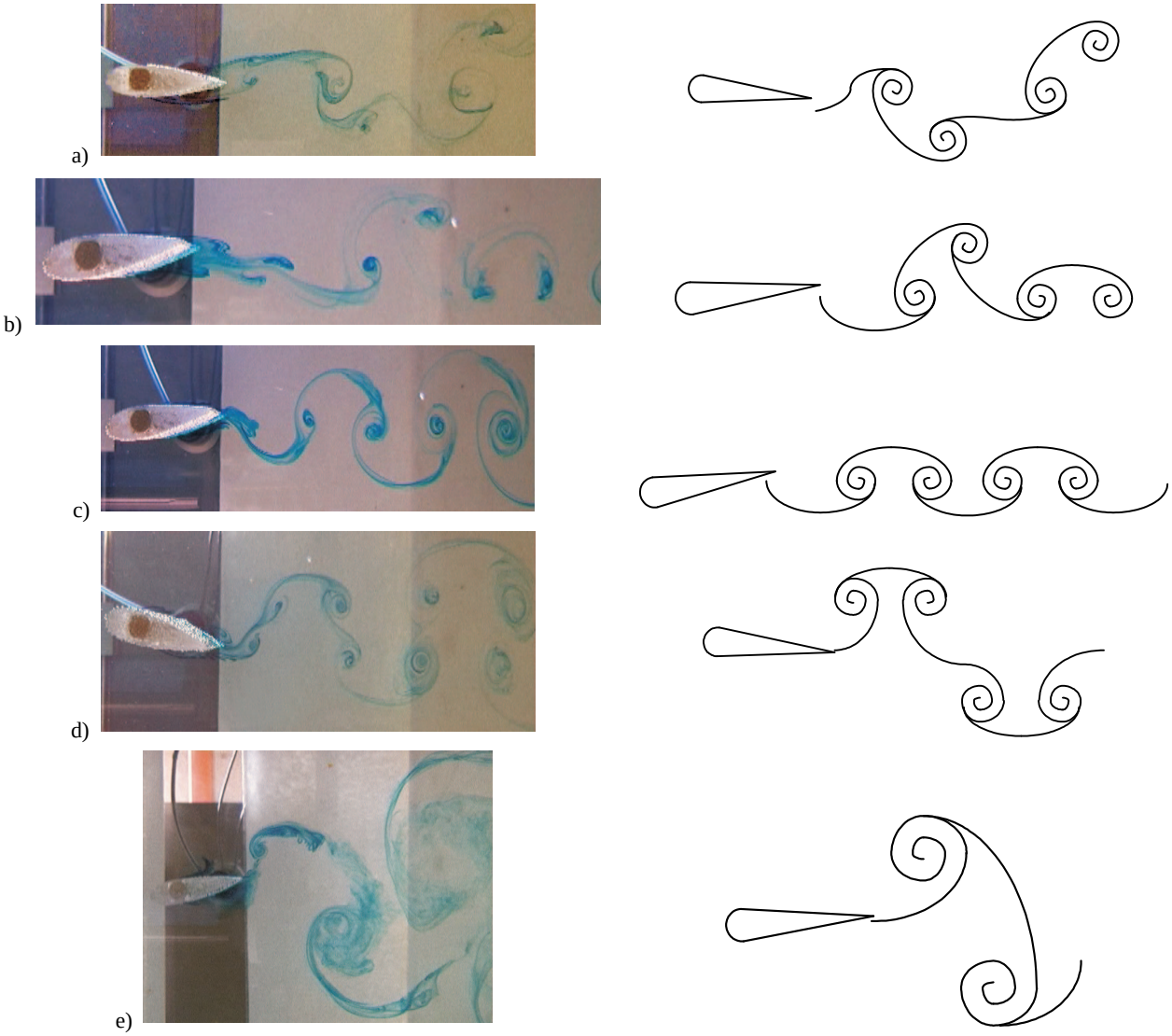

Figure 4: Vortex wake patterns. Flow is from left to right. Case a) Drag (St = 0.09) b) Drag (St = 0.12) c) In-line (St = 0.19) d) Vortex Pair (St = 0.23) e) Reverse Karman (St = 0.53).

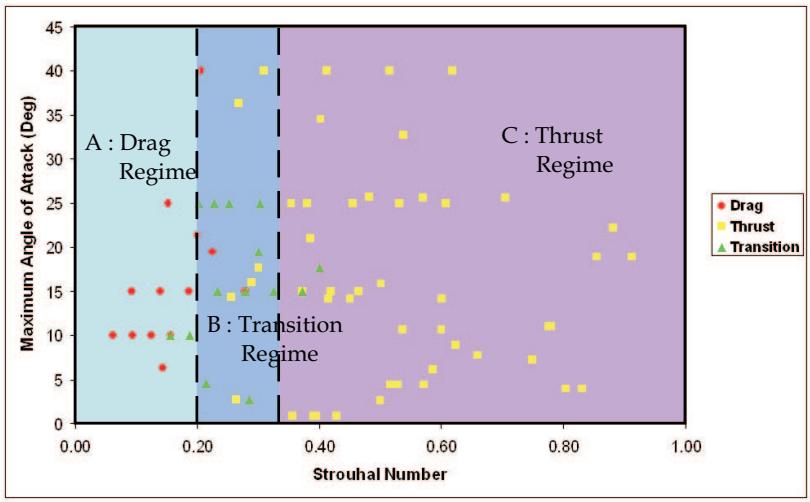

Figure 5: Vortex wake map.